THE JOURNAL OF BIOLOGICAL CHEMISTRY VOL. 291, NO. 40, pp. 21148–21159, September 30, 2016

Orai1 and TRPC1 Proteins Co-localize with $Ca_V1.2$ Channels to Form a Signal Complex in Vascular Smooth Muscle Cells*

Received for publication, June 10, 2016, and in revised form, July 28, 2016 Published, JBC Papers in Press, August 17, 2016, DOI 10.1074/jbc.M116.742171

Javier Ávila-Medina[‡§], Eva Calderón-Sánchez[§], Patricia González-Rodríguez[‡], Francisco Monje-Quiroga[¶], Juan Antonio Rosado[‖], Antonio Castellano[‡], Antonio Ordóñez[§], and Tarik Smani[‡§1]

From the [‡]Departamento de Fisiología Médica y Biofísica and [§]Grupo de Fisiopatología Cardiovascular, Instituto de Biomedicina de Sevilla (IBiS), Hospital Universitario Virgen del Rocío/CSIC/Universidad de Sevilla, 41013 Sevilla, Spain, the [¶]Department of Neurophysiology and Neuropharmacology, Center for Physiology and Pharmacology, Medical University of Vienna, 1090 Wien, Austria, and the [‖]Departamento de Fisiología, Universidad de Extremadura, 10071 Cáceres, Spain

Voltage-dependent $Ca_V1.2$ L-type Ca^{2+} channels (LTCC) are the main route for calcium entry in vascular smooth muscle cells (VSMC). Several studies have also determined the relevant role of store-operated Ca^{2+} channels (SOCC) in vascular tone regulation. Nevertheless, the role of Orai1- and TRPC1-dependent SOCC in vascular tone regulation and their possible interaction with $Ca_V1.2$ are still unknown. The current study sought to characterize the co-activation of SOCC and LTCC upon stimulation by agonists, and to determine the possible crosstalk between Orai1, TRPC1, and $Ca_V1.2$. Aorta rings and isolated VSMC obtained from wild type or smooth muscle-selective conditional $Ca_V1.2$ knock-out ($Ca_V1.2^{KO}$) mice were used to study vascular contractility, intracellular Ca^{2+} mobilization, and distribution of ion channels. We found that serotonin (5-HT) or store depletion with thapsigargin (TG) enhanced intracellular free Ca^{2+} concentration ($[Ca^{2+}]_i$) and stimulated aorta contraction. These responses were sensitive to LTCC and SOCC inhibitors. Also, 5-HT- and TG-induced responses were significantly attenuated in $Ca_V1.2^{KO}$ mice. Furthermore, hyperpolarization induced with cromakalim or valinomycin significantly reduced both 5-HT and TG responses, whereas these responses were enhanced with LTCC agonist Bay-K-8644. Interestingly, *in situ* proximity ligation assay revealed that $Ca_V1.2$ interacts with Orai1 and TRPC1 in untreated VSMC. These interactions enhanced significantly after stimulation of cells with 5-HT and TG. Therefore, these data indicate for the first time a functional interaction between Orai1, TRPC1, and $Ca_V1.2$ channels in VSMC, confirming that upon agonist stimulation, vessel contraction involves Ca^{2+} entry due to co-activation of Orai1- and TRPC1-dependent SOCC and LTCC.

Vasoactive agonists are known to promote vessel contraction by a rise in intracellular free Ca^{2+} concentration ($[Ca^{2+}]_i$). This increase in $[Ca^{2+}]_i$ has been classically considered to occur first, due to a rapid Ca^{2+} release from sarcoplasmic reticulum (SR)[2] stimulated by inositol 1,4,5-trisphosphate ($InsP_3$), and then to a transmembrane Ca^{2+} influx through L-type Ca^{2+} channels (LTCC), especially $Ca_V1.2$ channels, which are the main path for Ca^{2+} entry responsible for the excitation-contraction coupling process in excitable vascular smooth muscle cells (VSMC) (1). Other voltage-independent channels are also involved in transmembrane Ca^{2+} influx, such as store-operated Ca^{2+} channels (SOCC) responsible of extracellular Ca^{2+} entry, known as store-operated Ca^{2+} entry (SOCE) (2, 3). SOCC have been characterized both in freshly dispersed and in primary cultured VSMC from systemic and resistance vessels (4–6). It is well established that SOCE is mainly due to the activation of the Ca^{2+}-sensing regulatory protein stromal interaction molecule 1 (STIM1) and Orai1, the pore-forming subunit of SOCC in a wide range of non-excitable cells (7). Additionally, Orai1 was suggested to form a non-Ca^{2+} selective SOCC due to its association with TRPC1 in excitable cells (8, 9). Interestingly, evidence showed that TRPC1, Orai1, and $Ca_V1.2$ might interact with the proteins of other channels to form a signal complex in VSMC (10–12).

Taking into consideration that Ca^{2+} enters mainly through LTCC in VSMC, further understanding of how Orai1 and TRPC1 might influence the role of LTCC in Ca^{2+} signaling and contractility is needed to explain the physiological role of SOCC in vessel contraction, which still remains under debate (13). We hypothesized that Ca^{2+} release from the SR, induced by a vasoactive agonist such as serotonin (5-HT), could activate SOCE, leading to depolarization of the VSMC, which would stimulate LTCC. Therefore, the main aims of this study were first, to investigate whether SOCC activity might substitute LTCC function in VSMC, and second, to determine the endogenous distribution of Orai1, TRPC1, and $Ca_V1.2$ in VSMC.

* This work was supported by grants from the Spanish Ministry of Economy and Competitiveness (BFU2013-45564-C2-1-P; BFU2013-45564-C2-2-P); the Institute of Carlos III and Cardiovascular Network "RIC" (RD12/0042/0041; PI12/00941); and the Andalusia Government (PI-0108-2012; P12-CTS-1965). The authors declare that they have no conflicts of interest with the contents of this article.

[1] To whom correspondence should be addressed: Instituto de Biomedicina de Sevilla/Hospital Universitario Virgen del Rocío, Grupo de Fisiopatología Cardiovascular, Lab 113, Avd. Manuel Siurot s/n, Sevilla 41013, Spain. Tel.: 34-955923057; Fax: 34-955923101; E-mail: tasmani@us.es.

[2] The abbreviations used are: SR, sarcoplasmic reticulum; LTCC, L-type Ca^{2+} channel(s); SOCC, store-operated Ca^{2+} channel(s); SOCE, store-operated Ca^{2+} entry; VSMC, vascular smooth muscle cell(s); $InsP_3$, inositol trisphosphate; 2APB, 2-aminoethoxydiphenyl borate; 5-HT, serotonin; BayK, Bay-K-8644; GSK, GSK-7975A; ML-9, 1-(5-chloronaphthalen-1-yl) sulfonyl-1,4-diazepane; PLA, proximity ligation assay; SERCA, sarco-endoplasmic reticulum calcium ATPase; TG, thapsigargin; PS, physiological solution; SMA, smooth muscle actin; Nif, nifedipine; Caf, caffeine; Crom, cromakalim; WT, wild type; Gd^{3+}, gadolinium.

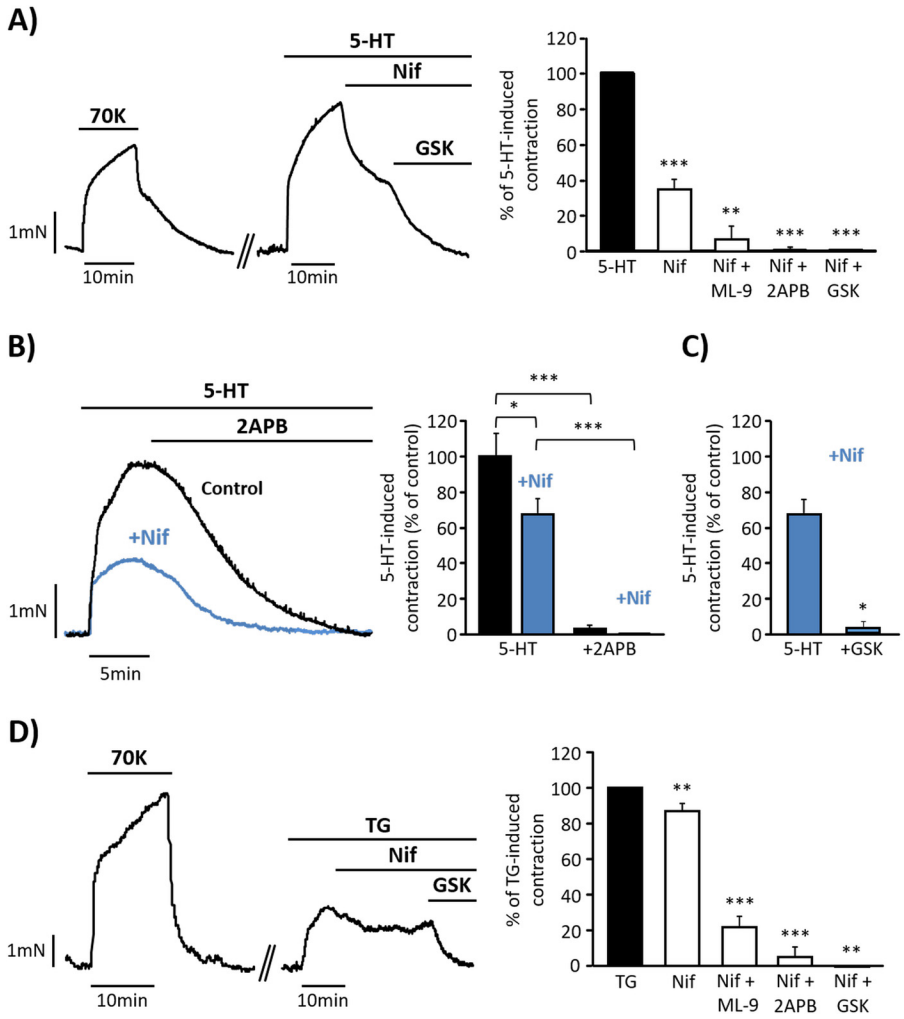

FIGURE 1. **Isometric contractions induced by serotonin and thapsigargin in mouse endothelium-denuded aorta.** *A*, representative recording showing high KCl (70 mM; *70K*) and 5-HT (10 μM) evoked contractions in endothelium-denuded mouse aorta. The cumulative addition of nifedipine (Nif, 1 μM) and GSK-7975A (GSK, 10 μM) fully relaxes 5-HT-induced contraction. GSK-7975A was substituted by 2APB (50 μM) or ML-9 (25 μM) in other experiments to inhibit SOCC. The *right panel* shows a data summary of the effects of Nif (34.08% $\pm$ 4.25; $n = 16$), Nif + ML-9 (7.28% $\pm$ 7.28; $n = 3$), Nif + 2APB (0.87% $\pm$ 0.65; $n = 8$), and Nif + GSK (0.57% $\pm$ 0.57; $n = 4$) on 5-HT-induced contraction (control; $n = 17$). *B*, representative traces and data summary showing 5-HT- (10 μM) induced contraction in control rings (*black bar* and *trace*; 100% $\pm$ 13.01; $n = 10$) and rings pre-treated with 1 μM Nif for 10 min (*blue trace* and *bars*; 69.30% $\pm$ 8.45; $n = 16$). 50 μM 2APB was added as indicated in control (3.13% $\pm$ 2.40) and in rings pretreated with nifedipine (0.18% $\pm$ 0.13). Values were normalized to 70K responses. *C*, data summary showing 5-HT- (10 μM) induced contraction in rings pre-treated with 1 μM nifedipine (69.31% $\pm$ 8.45; $n = 16$) and after GSK-7975A (10 μM) administration in rings pretreated with Nif (3.20% $\pm$ 3.20; $n = 3$). *D*, representative recording and data summary of 10 μM TG- ($n = 20$) elicited aorta contraction. 1 μM Nif (86.05% $\pm$ 3.84; $n = 22$) was added followed by GSK (0% $\pm$ 0; $n = 3$), 50 μM 2APB (5.37% $\pm$ 5.37; $n = 7$), or 50 μM ML-9 (21.97% $\pm$ 6.20; $n = 12$). Values are the percentage of mean $\pm$ S.E. *, $p < 0.05$, **, $p < 0.01$ and ***, $p < 0.001$.

Results

Agonist-induced Vasoconstriction Involves Ca^{2+} Entry through SOCC and LTCC in Endothelium-denuded Mouse Aorta—The role of SOCC and LTCC in contractile responses of aorta was studied using 5-HT as vasoactive agonist. Fig. 1*A* shows that 5-HT (10 μM) evoked a potent vasoconstriction in endothelium-denuded aorta, which was partially inhibited by nifedipine (1 μM), a specific inhibitor of LTCC in VSMC (14). The cumulative addition of GSK-7975A (10 μM), considered a specific inhibitor of Orai1 (15), further produced the complete relaxation of the vessel. Similar effects were also observed when other less specific inhibitors of SOCE, 2APB (50 μM) or ML-9 (25 μM) (3), were added after nifedipine, as summarized in Fig. 1*A*. Additionally, pre-treatment of aortic rings with 1 μM nifedipine attenuated but did not prevent 5-HT responses (Fig. 1, *B* and *C*); meanwhile the supplementary addition of 2APB (50 μM) or GSK-7975A (10 μM, Fig. 1*C*) produced the complete relaxation of the vessel. As shown in Fig. 1*B*, the addition of 2APB alone (50 μM) promoted the full relaxation of 5-HT-induced contraction, in contrast to the effect of nifedipine (Fig. 1*A*). Interestingly, the specific activation of SOCC with thapsigargin (TG, 10 μM), a SERCA inhibitor (16), evoked a nifedipine- (1 μM) sensitive vasoconstriction, although the inhibitory effect of nifedipine was smaller in comparison with its effect on 5-HT responses (Fig. 1*D*). Further relaxation was also produced by the addition of GSK-7975A (10 μM), 2APB (50 μM), or ML-9 (50 μM), indicating that TG-induced vasoconstriction involves LTCC and SOCC co-activation.

In experiments performed in isolated VSMC, administration of 5-HT (10 μM), applied in the continuous presence of extracellular Ca^{2+}, evoked a transient followed by a sustained elevation of $[Ca^{2+}]_i$ (Fig. 2*A*). Both fast and sustained 5-HT-induced

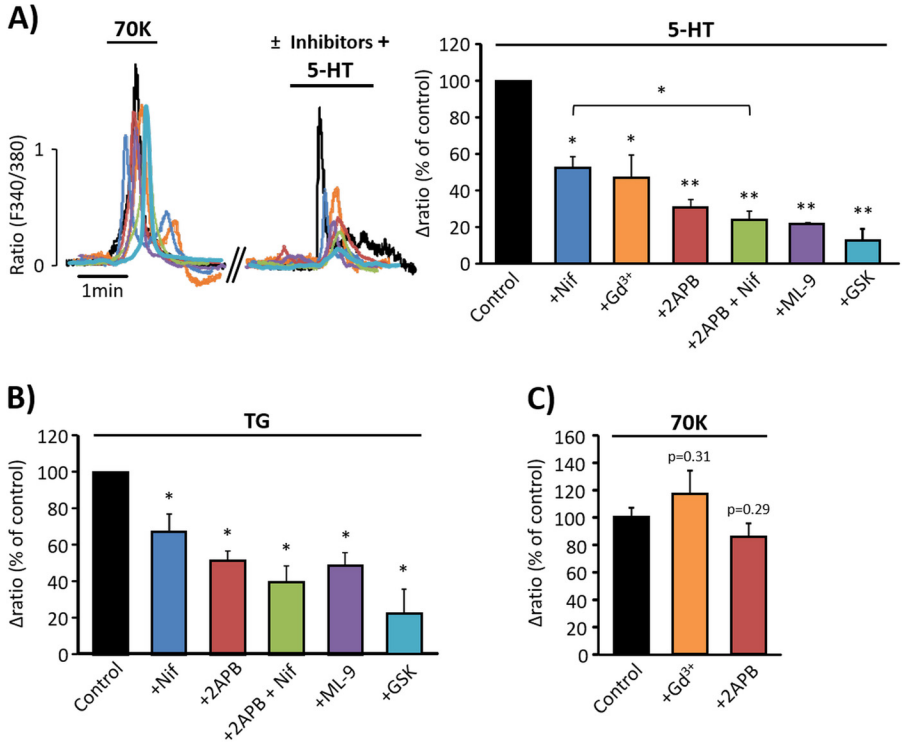

FIGURE 2. **$[Ca^{2+}]_i$ changes elicited by serotonin and thapsigargin in vascular smooth muscle cell.** *A*, *left panel*, representative traces of $[Ca^{2+}]_i$ responses in VSMC presented as fura-2 ratio (F_{340}/F_{380}). High KCl (70 mM; *70K*) was applied, and then 5-HT (10 μM) was added in the presence or absence of inhibitors. In the *right panel*, the bar graph summarizes 5-HT-evoked $[Ca^{2+}]_i$ increases in untreated cells (control, $n = 486$) and cells pre-treated with 100 nM Nif (52.30% ± 6.20; $n = 65$), 5 μM Gd^{3+} (47.15% ± 12.40; $n = 48$), 25 μM 2APB (30.69% ± 4.40; $n = 111$), 25 μM 2APB + 100 nM Nif (23.89% ± 5.00; $n = 96$), 25 μM ML-9 (21.67% ± 0.50; $n = 102$), and 5 μM GSK (12.67% ± 6.53; $n = 160$). *B*, relative data summary of TG- (2 μM) induced $[Ca^{2+}]_i$ changes in VSMC ($n = 379$) and in cells pre-treated with 100 nM Nif (67.51% ± 9.66; $n = 141$), 25 μM 2APB (51.49% ± 5.45; $n = 148$), 25 μM 2APB + 100 nM Nif (39.86% ± 8.89; $n = 120$), 10 μM ML-9 (48.70% ± 7.36; $n = 110$), and 5 μM GSK (22.10% ± 13.71; $n = 152$). *C*, data summary of $[Ca^{2+}]_i$ increases evoked by 70K in VSMC (100% ± 7.86; $n = 85$) or in the presence of 5 μM Gd^{3+}(105.18% ± 15.31; $n = 27$) and 50 μM 2APB (76.74% ± 9.15; $n = 88$). Values are the percentage of mean ± S.E. normalized to the first response to 70K from at least 3 different experiments. *, $p < 0.05$, **, $p < 0.01$ *versus* control.

$[Ca^{2+}]_i$ increases were sensitive to nifedipine (100 nM) and to the SOCC inhibitors, GSK-7975A (5 μM), Gd^{3+} (5 μM), 2APB (25 μM), and ML-9 (10 μM). Pre-treatment of cells with 2APB (25 μM) together with nifedipine (100 nM) caused significantly stronger suppression of 5-HT-evoked $[Ca^{2+}]_i$ responses, as compared with the effect of nifedipine alone. Similarly, the addition of TG (2 μM) in the presence of extracellular Ca^{2+} induced an increase in $[Ca^{2+}]_i$, which was sensitive to nifedipine (100 nM), GSK-7975A (5 μM), 2APB (25 μM), and ML-9 (10 μM), as shown in Fig. 2*B*. The effect of 2APB (25 μM) applied together with nifedipine (100 nM) caused additional reduction of TG-evoked $[Ca^{2+}]_i$ increase, like their effects in 5-HT response. In similar experiments, we tested a higher concentration of nifedipine (500 nM), and the effects were not significantly different from those obtained using 100 nM (data not shown). Fig. 2*C* shows data from control experiments in which Gd^{3+} (5 μM) and 2APB (50 μM) did not affect high KCl-induced $[Ca^{2+}]_i$ responses. Altogether, these data suggest that 5-HT- and TG-induced $[Ca^{2+}]_i$ increase and artery vasoconstriction involve Ca^{2+} entry through both LTCC and SOCC.

SOCE Does Not Compensate LTCC Function in Endothelium-denuded Aorta of $Ca_V1.2$ Knock-out Mice—Next, we examined whether SOCC can substitute LTCC function in vascular tone regulation. We used aorta from a conditional $Ca_V1.2$ knock-out ($Ca_V1.2^{KO}$) mouse model to assess 5-HT and TG effects. Fig. 3*A* indicates that $Ca_V1.2$ protein expression was efficiently decreased in $Ca_V1.2^{KO}$ mice as compared with wild type (WT). Consistently, aorta contraction induced by depolarizing stimulus, high KCl (70 mM), was significantly attenuated in $Ca_V1.2^{KO}$ mice as compared with WT (Fig. 3, *B* and *F*). In the same way, 5-HT (10 μM, Fig. 3, *C* and *F*) and TG (10 μM, Fig. 3, *D* and *F*) induced significantly smaller contractions in $Ca_V1.2^{KO}$ aorta as compared with WT. 5-HT- and TG-evoked vasoconstrictions in $Ca_V1.2^{KO}$ aorta were still somewhat sensitive to nifedipine (1 μM), probably due to the presence of the remaining functional $Ca_V1.2$ channels (Fig. 3, *C–H*). Interestingly, the evoked contractions were largely inhibited by 2APB (50 μM) or ML-9 (25 μM), as shown in Fig. 3, *C* and *D* and summarized in Fig. 3, *G* and *H*. Moreover, in freshly isolated $Ca_V1.2^{KO}$ VSMC, the addition of high KCl, 5-HT (10 μM), or TG (2 μM) evoked significantly reduced $[Ca^{2+}]_i$ responses, as compared with WT (Fig. 4, *A–C*). Because the effect of vasoconstrictor agonists depends on the initial $InsP_3$-induced Ca^{2+} release from intracellular stores, we checked the integrity of the SR in $Ca_V1.2^{KO}$ mice using caffeine, to release Ca^{2+} from ryanodine-sensitive stores (17). We observed that vessel contractions (Fig. 3, *E* and *F*) and $[Ca^{2+}]_i$ increases (Fig. 4, *A* and *C*) induced by caffeine (10 mM) stimulation were not affected in $Ca_V1.2^{KO}$ mice, confirming that 5-HT- and TG-reduced responses are not due to differences in SR Ca^{2+} load between WT and $Ca_V1.2^{KO}$ mice.

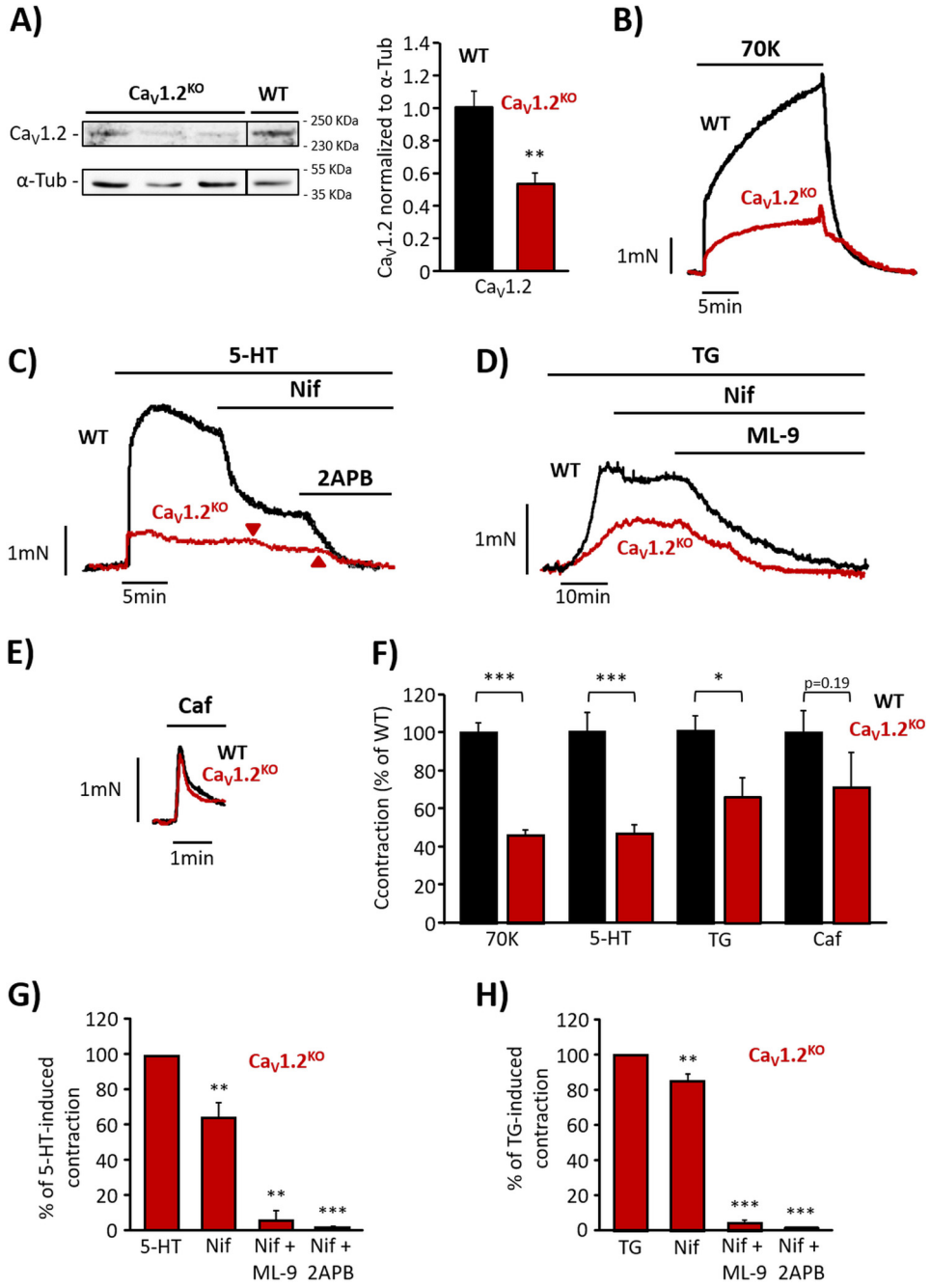

FIGURE 3. **Effect of serotonin in endothelium-denuded aorta isolated from $Ca_V1.2$ knock-out mice.** *A*, Western blots and data summary of $Ca_V1.2$ protein expression in wild type (WT, 1.00 ± 0.10; $n = 4$) and $Ca_V1.2$ knock-out mice ($Ca_V1.2^{KO}$, 0.59 ± 0.06; $n = 4$). *α-Tub*, α-tubulin. *B*, representative traces of aortic ring contractions induced by high KCl (70 mM; *70K*) in aorta from WT and $Ca_V1.2^{KO}$ mice. *C*, representative recordings showing 5-HT- (10 μM) evoked contraction and the effects of the addition of nifedipine (Nif, 1 μM) and 2APB (50 μM) in aortic rings from WT and $Ca_V1.2^{KO}$ mice. The *arrows* indicate the time when nifedipine and 2APB were applied in $Ca_V1.2^{KO}$ aortic ring. *D*, representative traces of TG- (10 μM) evoked contraction and the effects of the cumulative addition of nifedipine (1 μM) and ML-9 (25 μM) in aortic rings from WT and $Ca_V1.2^{KO}$ mice. *E*, representative contraction of aortic rings from WT and $Ca_V1.2^{KO}$ mice induced by caffeine (Caf, 10 mM) *F*, data summary of aortic ring contractions induced by 70K, 5-HT, TG, and Caf from WT (*black bars*; 70K, 100% ± 5.58; 5-HT, 100% ± 11.23; TG, 100% ± 10.95; Caf, 100% ± 12.10; $n = 11–42$) and $Ca_V1.2^{KO}$ mice (*red bars*; 70K, 51.24% ± 3.17; 5-HT, 46.02% ± 6.42; TG, 66.23% ± 10.22; Caf, 71% ± 18.68; $n = 10–31$). *G*, data summary of 5-HT-induced contractions from $Ca_V1.2^{KO}$ aorta ($n = 11$) and the effects of 1 μM Nif (64.16% ± 8.70; $n = 10$), 1 μM Nif + 50 μM 2APB (1.34% ± 0.63; $n = 6$), or 1 μM Nif + 25 μM ML-9 (5.61% ± 5.61; $n = 3$). *H*, data summary showing the effects of 1 μM Nif (85.14% ± 4.15; $n = 12$), 1 μM Nif + 50 μM 2APB (0.83% ± 0.83; $n = 5$), and 1 μM Nif + 50 μM ML-9 (4.42% ± 1.93; $n = 7$) on TG-induced aorta contractions from $Ca_V1.2^{KO}$ mice ($n = 13$). Values are the percentage of mean ± S.E. *, $p < 0.05$, **, $p < 0.01$, and ***, $p < 0.001$.

Effects of Membrane Potential Manipulation on 5-HT and TG Responses—In light of the previous data demonstrating that 5-HT and TG co-activate SOCC and LTCC, we examined whether changes in membrane potential are relevant for the responses to agonists. Therefore, we tested the effect of cromakalim, an agonist of ATP-sensitive K^+ channel (K_{ATP}) widely used to promote significant hyperpolarization (18). Fig. 5, *A* and *B*, show that aorta pre-treatment with cromakalim (20 μM) significantly reduced 5-HT- (10 μM) and TG- (10 μM) induced vasoconstriction, whereas pre-treatment of vessels

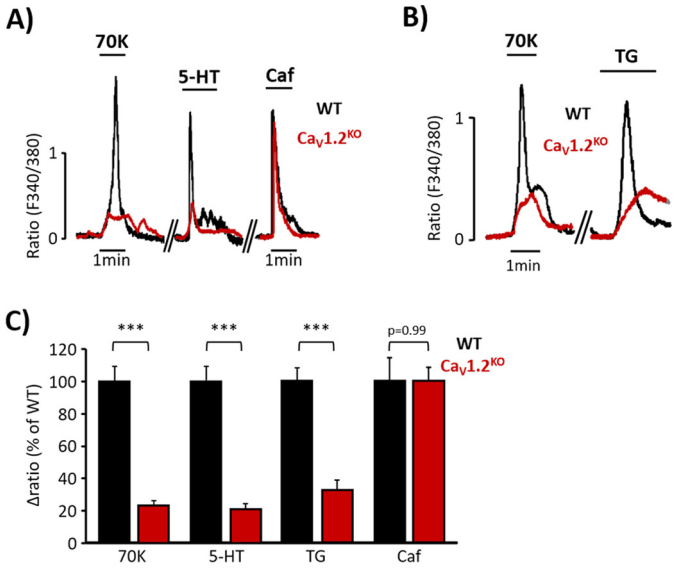

FIGURE 4. **$[Ca^{2+}]_i$ increases elicited by serotonin or thapsigargin are diminished in $Ca_V1.2^{KO}$ mice.** *A*, representative $[Ca^{2+}]_i$ changes in aortic VSMC from wild type (WT, *black traces*) and $Ca_V1.2$ knock-out mice ($Ca_V1.2^{KO}$, *red traces*) mice evoked by high KCl (70 mM; *70K*), 5-HT (10 μM), and Caf (10 mM). *B*, representative $[Ca^{2+}]_i$ changes of aortic VSMC from WT (*black traces*) and $Ca_V1.2^{KO}$ (*red traces*) mice evoked by 70K and TG (10 μM). *C*, data summary of $[Ca^{2+}]_i$ changes induced by 70K, 5-HT, TG, and Caf in VSMC from WT (*black bars*; 70K, 100% ± 8.77; 5-HT, 100% ± 13.18; TG, 100% ± 8.57; Caf, 100% ± 14.23; n = 379–1157) and $Ca_V1.2^{KO}$ mice (*red bars*; 70K, 22.92% ± 2.82; 5-HT, 20.76% ± 3.94; TG, 26.83% ± 6.18; Caf, 99.88% ± 8.60; n = 190–640). Values are the percentage of mean ± S.E. ***, $p < 0.001$ *versus* control.

with glibenclamide (3 μM), an inhibitor of K_{ATP} channel (14) that blocks the hyperpolarizing action of cromakalim, efficiently antagonized its effects on 5-HT-induced contraction (Fig. 5*A*). Moreover, the increase in $[Ca^{2+}]_i$ induced by both 5-HT (Fig. 5*C*) and TG (Fig. 5*D*) in isolated VSMC was also inhibited by cromakalim (5 μM). Nevertheless, the responses to high KCl or caffeine were not significantly affected by the application of cromakalim neither in aortic rings (Fig. 5*E*) nor in isolated VSMC (Fig. 5*F*). To confirm these findings, we explored the effect of valinomycin, a potassium-selective ionophore that promotes hyperpolarization, bringing the membrane potential to values close to the Nernst potential for potassium (19). As shown in Fig. 6, *A* and *B*, pre-treatment of aortic rings with valinomycin (500 nM) significantly reduced the effects of 5-HT and TG on vasoconstriction. In addition, incubation of VSMC with valinomycin (100 nM) significantly inhibited 5-HT- (Fig. 6*C*) and TG- (Fig. 6*D*) evoked $[Ca^{2+}]_i$ increase, whereas the high KCl and caffeine responses were not affected.

To corroborate the physiological relevance of the co-activation of LTCC and SOCC during agonist stimulation, we explored whether LTCC agonist Bay-K-8644 (BayK) (20) could enhance aorta responses elicited by 5-HT and TG. As shown in Fig. 7, *A* and *B*, aortic rings pre-treated with BayK (100 nM) exhibited significantly higher contractions when stimulated with 5-HT and TG as compared with untreated aortic rings. The addition of 2APB (50 μM) efficiently relaxed 5HT- and TG-induced vasoconstriction in BayK-treated arterial rings. Similar increased responses were also observed when high KCl was applied in BayK-treated aorta (Fig. 7*C*).

Altogether, these data suggest that vasoconstrictions initiated by 5-HT or SOCE activation with TG are attenuated in hyperpolarized arteries, whereas these responses are potentiated when the LTCC activation threshold is shifted toward hyperpolarized potentials.

Endogenous Distribution of Orai1, TRPC1, and $Ca_V1.2$ in VSMC—Orai1 and TRPC1 are suggested to interact to form non-selective SOCC in VSMC (8). Several lines of evidence suggest that the $Ca_V1.2$ isoform might form a different signal complex with other channels to handle $[Ca^{2+}]_i$ in VSMC (10–12). Here, we examined the endogenous subcellular localization of $Ca_V1.2$, Orai1, and TRPC1 and their possible interaction by the *in situ* proximity ligation assay (PLA). Fig. 8, *A* and *C*, show a large number of PLA red puncta in VSMC when incubated with primary antibodies against $Ca_V1.2$ and Orai1. Meanwhile, no PLA signal was detected in VSMC conjugated only with anti-Orai1 antibody, but without anti-$Ca_V1.2$ antibody (Fig. 8, *B* and *C*). Similarly, Fig. 9*A* shows that $Ca_V1.2$ interacts with TRPC1, as indicated by a large number of red PLA puncta in VSMC. Interestingly, VSMC stimulation with 5-HT (10 μM) and TG (2 μM), but not with high KCl, significantly increased puncta signals, indicating a significant rise in the interaction of $Ca_V1.2$ with Orai1 (Fig. 8, *A* and *C*) and TRPC1 (Fig. 9, *A* and *C*) after agonist stimulation. These data suggest that Orai1 and TRPC1 interact with $Ca_V1.2$ in basal conditions and upon agonist stimulation, which will certainly favor their functional communication upon agonist stimulation to promote intracellular Ca^{2+} signaling in VSMC.

Discussion

Although it is widely accepted that LTCC and SOCC contribute to the physiopathology of VSMC, their direct functional relationship had remained virtually unexplored. The present study provides new data confirming the role of SOCC in vascular tone regulation, unveiling for the first time a functional crosstalk between $Ca_V1.2$, Orai1, and TRPC1 channels that might serve for fine-tuning of vascular smooth muscle Ca^{2+} signaling, as summarized in the scheme shown in Fig. 10. Routinely, to activate SOCE, pharmacological or physiological agonists were added in the absence of Ca^{2+}, and then extracellular Ca^{2+} was restored in the well known "Ca^{2+}-free/Ca^{2+}-readmission" or "Ca^{2+} add-back" protocols (see for example Ref. 5). Nevertheless, there is little information about physiological agonists that can activate SOCE in the continuous presence of extracellular Ca^{2+}, without store depletion, as discussed elsewhere (13). In this study, we demonstrated that 5-HT applied in the presence of extracellular Ca^{2+} evoked a fast increase of $[Ca^{2+}]_i$, followed by a sustained phase, in isolated VSMC. 5-HT also activated a sustained vasoconstriction in aortic rings. These responses were sensitive to inhibitors of SOCC, supporting the involvement of SOCE in vessel contraction. In fact, we showed that GSK-7975A, which is considered a specific inhibitor of Orai1 (15), as well as other blockers, efficiently inhibited 5-HT-induced responses. Gd^{3+}, 2APB, and ML-9 are still widely used as SOCE inhibitors in different cell types (3), despite their lack of specificity. In this study, the involvement of SOCC in vasoconstriction is also supported by the specific activation with TG, which induced aorta vasoconstriction, indicating that SOCE contributes to vascular tone regulation, in agreement with previous studies (21, 22). Interestingly, we also

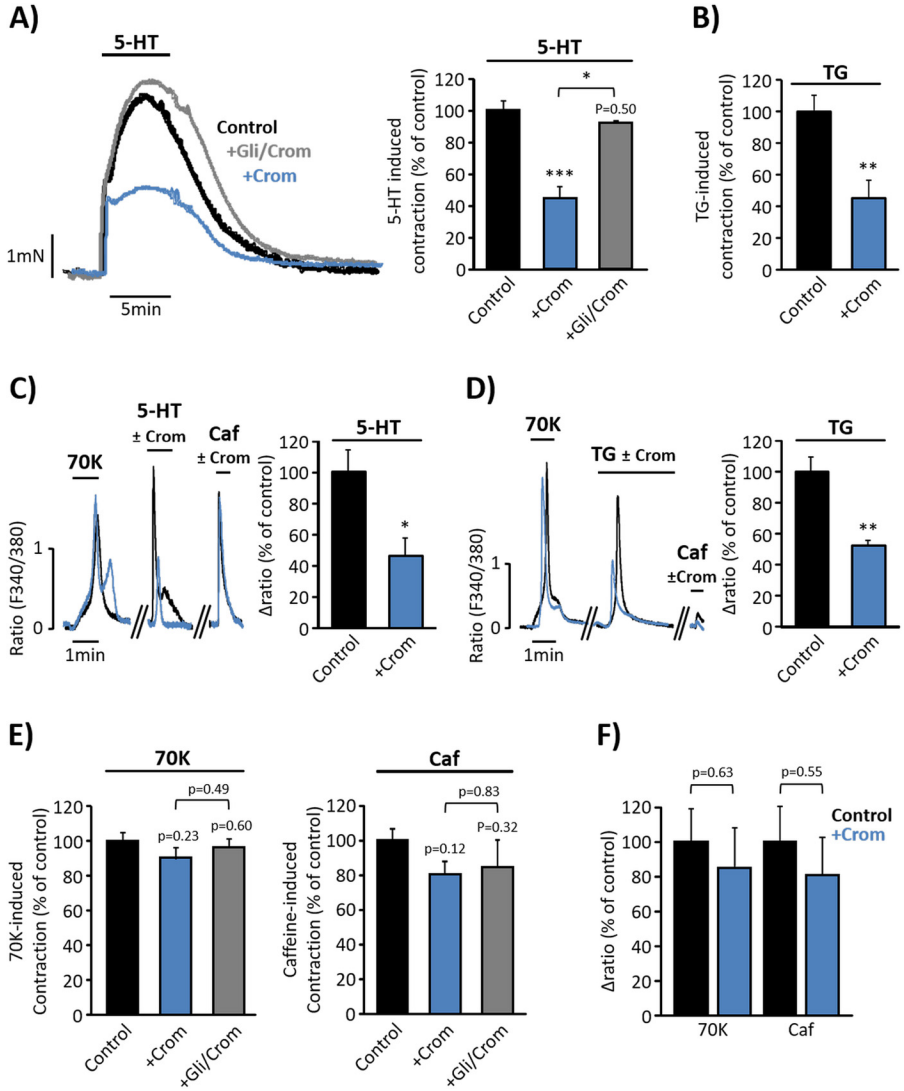

FIGURE 5. **Cromakalim attenuates serotonin and thapsigargin responses.** *A*, representative traces and data summary of 5-HT- (10 μM) evoked contraction in aortic rings pre-incubated for 15 min with vehicle (control, *black trace* and *bar*; 100% ± 5.73; $n = 6$), with 20 μM cromakalim (+Crom; *blue trace* and *bar*; 44.59% ± 7.16; $n = 3$) or with 3 μM glibenclamide together with 20 μM cromakalim (+*Gli/Crom*, *gray trace* and *bar*; 92.47% ± 0.72; $n = 3$). *B*, data summary of TG- (10 μM) induced contraction in aortic rings pre-incubated for 15 min with vehicle (control, 100% ± 9.70; $n = 4$) or 20 μM Crom (45.15% ± 10.86; $n = 4$). *C*, representative traces of $[Ca^{2+}]_i$ changes elicited by high KCl (70 mM, *70K*), 10 μM 5-HT, and 10 mM Caf in VSMC pre-incubated for 3 min with vehicle (control, *black trace* and *bar*), or with 5 μM Crom (*blue trace* and *bar*). Data summaries of 5-HT responses in the presence of vehicle (control, 100% ± 14.44; $n = 79$) and in the presence of Crom (46.39% ± 10.94; $n = 87$) are shown. *D*, representative traces of $[Ca^{2+}]_i$ changes elicited by 70K, 2 μM TG, and 10 mM Caf in VSMC pre-incubated for 3 min with vehicle (control, *black trace* and *bar*), or with 5 μM Crom (*blue trace* and *bar*). Data summaries of $[Ca^{2+}]_i$ changes elicited by 2 μM TG applied in control (100% ± 9.30, $n = 151$) or in the presence of cromakalim (52.36% ± 2.95, $n = 94$) are shown. *E*, bar graphs summarize 70K- and caffeine-induced vasoconstriction in control (70K = 100% ± 4.33 and Caf = 100% ± 6.80; $n = 6$), in rings pretreated for 15 min with 20 μM Crom (70K = 90.09% ± 6.39 and Caf = 80.44% ± 7.68; $n = 3$), and in rings treated for 15 min with 3 μM glibenclamide + 20 μM cromakalim (+*Gli/Crom*; 70K = 96.13% ± 5.00; Caf = 84.42% ± 16.32; $n = 3$). *F*, data summary of $[Ca^{2+}]_i$ changes produced by 70K and Caf (10 mM) in VSMC pre-treated for 3 min with vehicle (control, 70K = 100% ± 18.67 and Caf = 100% ± 20.13; $n = 95$), or with 5 μM Crom (70K = 84.97% ± 22.55 and Caf = 80.91% ± 21.81; $n = 74$). Values are the percentage of mean ± S.E. normalized to 70K responses. *, $p < 0.05$, **, $p < 0.01$, and ***, $p < 0.001$.

demonstrated that SOCC sustained Ca^{2+} entry and vasoconstriction in $Ca_V1.2^{KO}$ mice, although not enough to completely compensate for the absence of functional LTCC. Our results using the $Ca_V1.2^{KO}$ mice confirmed the requirement of functional LTCC for vessel contraction even when vasoconstriction was specifically activated through SOCE using TG. These data agree with previous studies using $Ca_V1.2^{KO}$ mice, which demonstrated that $Ca_V1.2$ is essential to control blood pressure and vasoconstrictor responses (17, 23).

Furthermore, increasing lines of evidence suggested that SOCE activation could serve not only as an important path for Ca^{2+} entry, but also as a depolarizing trigger for a secondary activation of LTCC in VSMC (24). Knowing that sarcolemmal K^+ channels are key regulators of resting potential in VSMC and vascular tone (25), we demonstrated that 5-HT and TG responses were sensitive to membrane potential changes, as they were attenuated by cromakalim or valinomycin, suggesting a smaller contribution of LTCC under these conditions. Valinomycin is expected to maintain the driving force for Ca^{2+} entry upon SOCE activation, as it impairs membrane depolarization. This might result in a slight increase in Ca^{2+} entry via SOCE, which, in our hands did not compensate for the effect of

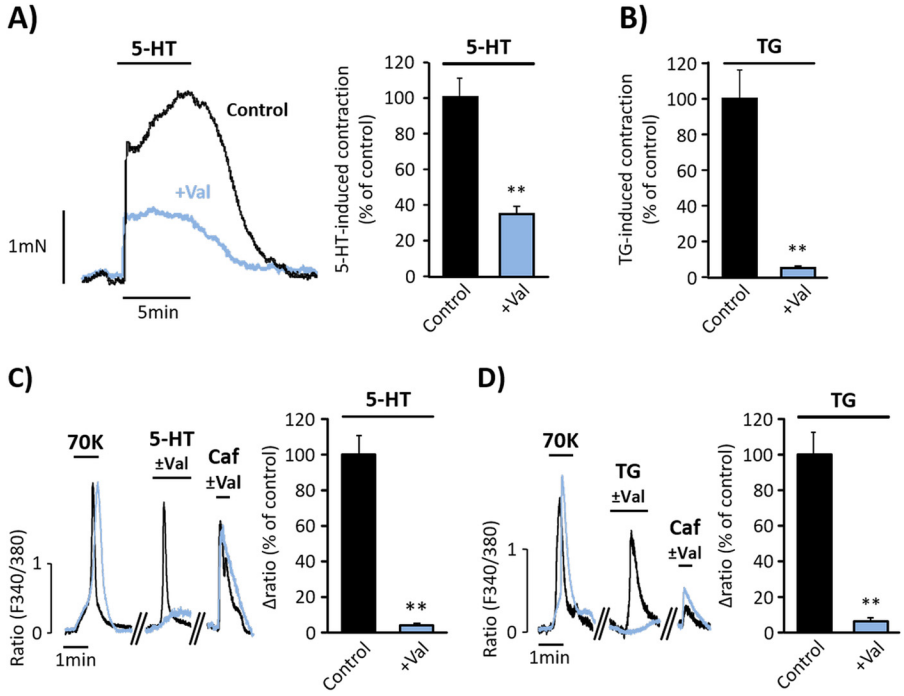

FIGURE 6. **Valinomycin attenuates serotonin- and thapsigargin-induced vasoconstriction and $[Ca^{2+}]_i$ increase.** *A* and *B*, representative traces and data summary of 5-HT- (10 μM) and TG- (10 μM) evoked contractions in control aortic rings (in *black*; 5-HT = 100% ± 10.62, $n = 9$; and TG = 100% ± 16.07; $n = 5$), and in rings pre-incubated for 15 min with 500 nM valinomycin (+*Val*, in *blue*; 5-HT = 35.10% ± 4.67, $n = 4$ and TG = 5.57% ± 0.53, $n = 3$). *C* and *D*, representative traces and data summary of $[Ca^{2+}]_i$ changes elicited by high KCl (*70K*, 70 mM) 10 μM 5-HT, and 2 μM TG and in control VSMC (5-HT = 100% ± 11.24, $n = 93$ and TG = 100% ± 12.64, $n = 90$) and in cells pre-incubated for 3 min with 100 nM valinomycin (5-HT = 3.68% ± 0.63, $n = 89$ and TG = 6.38% ± 1.95, $n = 114$). 10 mM Caf was applied at the end of each experiment as indicated. Values are the percentage of mean ± S.E. normalized to 70K responses. **, $p < 0.01$.

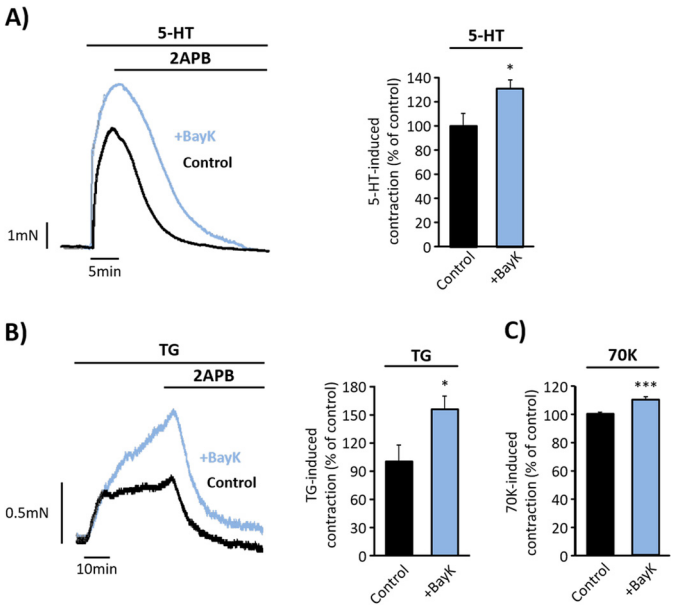

FIGURE 7. **LTCC agonist, BayK, increases endothelium-denuded aorta responses.** *A* and *B*, representative traces and data summary of 5-HT- (10 μM) and TG- (10 μM) evoked contractions in control aortic rings (in *black*; 5-HT = 100% ± 10.53, $n = 3$; and TG = 100% ± 17.57, $n = 6$) and in rings pre-incubated for 15 min with 100 nM BayK (in *blue*; 5-HT = 131.30% ± 7.16, $n = 4$ and TG = 155% ± 13.65, $n = 5$). 2APB (50 μM) was added as indicated. *C*, bar graph shows a data summary of high KCl (*70K*, 70 mM) responses in control rings (100% ± 1.55, $n = 11$) and in rings pre-incubated with BayK for 15 min (110% ± 1.83, $n = 12$). Values are the percentage of mean ± S.E. normalized to 70K responses. *, $p < 0.05$, ***, $p < 0.001$.

the secondary activation of LTCC. To our knowledge, few studies have suggested that hyperpolarization, due to K_{Ca} channel activation, sustained Ca^{2+} entry through SOCE (for example, in chondrocytes) (26). On the other hand, BayK, which shifts LTCC activation to hyperpolarized potentials, enhanced agonist responses. Thus, our results indicated that agonist responses can be attenuated or potentiated significantly depending on the open probability of LTCC. Similarly, a recent study demonstrated that depletion of SR stimulated SOCE, producing depolarization and LTCC activation in rat myometrium (27). Recently, we have determined that the transient expression of $Ca_V1.2$ channel subunits in HEK cells resulted in a significant increase in Ca^{2+} entry induced by TG, attributed to secondary activation of $Ca_V1.2$ channels induced by cation influx via SOCC (28). We have also demonstrated that upon store depletion, STIM1 inhibits Ca^{2+} entry through LTCC (28), in agreement with studies by other groups (29). Our data suggest that store depletion might promote two independent mechanisms involving the interaction of different components of SOCE with $Ca_V1.2$ to fine-tune its activity: Ca^{2+} influx via SOCE promotes secondary activation of LTCC, and STIM1 modulates $Ca_V1.2$ function. Certainly, further investigations are needed to shed more light on this intriguing reciprocal regulation of LTCC by store depletion. In fact, the dual regulation of LTCC by $[Ca^{2+}]_i$ increase has been extensively studied in excitable cells, as reviewed recently (30). $[Ca^{2+}]_i$ enhancement is known to promote the well characterized Ca^{2+}-dependent inactivation process likely to prevent Ca^{2+} overload (31), whereas $[Ca^{2+}]_i$ increase can also stimulate Ca^{2+}-dependent facilitation of $Ca_V1.2$ to potentiate Ca^{2+} influx, for example, during the excitation-contraction coupling in VSMC (32).

Another important issue that remains under debate is the identity of SOCC in excitable VSMC. Several groups have

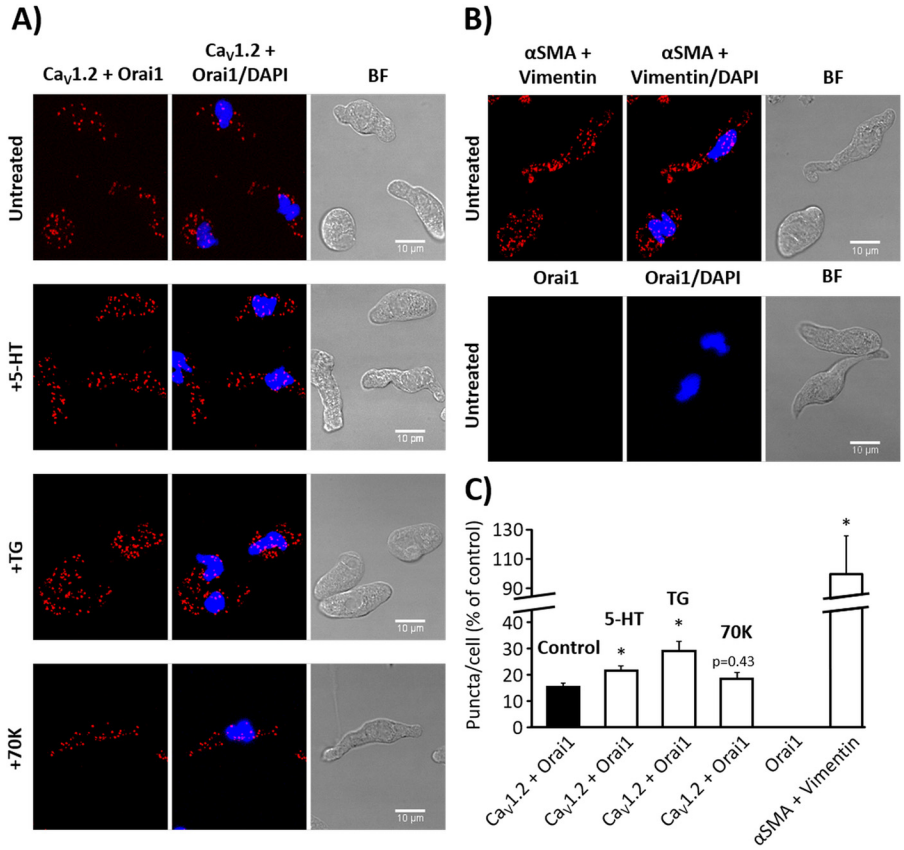

FIGURE 8. **Orai1 and $Ca_V1.2$ co-localization in aortic myocytes.** *A*, representative images of aortic VSMC using primary antibodies against $Ca_V1.2$ and Orai1 conjugated with the appropriate PLA probes, from untreated control cells or from cells stimulated with 5-HT (10 μM), TG (2 μM), or high KCl (*70K*, 70 mM). *Red puncta* indicate that proteins are in close proximity (<40 nm). The *left panels* show VSMC images when antibodies were conjugated with PLA probes, the *middle panels* show merges images from cells also stained with DAPI (*blue*), and the *right panels* show bright field (*BF*) pictures. *B*, images from VSMC using primary antibodies against α-SMA and vimentin used as positive control (*upper panel*) and from VSMC conjugated with only anti-Orai1 primary antibody as negative control (*lower panel*). *C*, the bar graph summarizes the mean number of PLA signals in untreated control VSMC (15.42% ± 1.50; $n = 6$), and in VSMC stimulated with 5-HT (21.60% ± 1.65; $n = 10$), TG (28.90% ± 3.81; $n = 8$), or 70K (18.33% ± 2.45; $n = 8$). No detectable PLA puncta were observed in control experiments using cells conjugated only with anti-Orai1 antibody (*Orai1*, $n = 8$). The interaction between anti-α-SMA and anti-vimentin antibodies was used as positive control (100% ± 25.88; $n = 5$). Similar experiments were repeated 3 times. Values are the percentage of mean ± S.E., normalized to positive control. Significance values indicate difference as compared with control, *, $p < 0.05$.

shown interactions between different proteins to form the SOCE signaling complex as discussed elsewhere (33, 34). Here, using *in situ* PLA assay, we showed for the first time that endogenous Orai1, TRPC1, and $Ca_V1.2$ are distributed in close vicinity. Indeed, hybridization of the PLA probes that occurs when proteins are <40 nm apart (35) confirmed a strong co-localization between these channels. Remarkably, we observed a significant increase of puncta signals in cells incubated with agonists that involve SOCE activation (5-HT through the $InsP_3$ signaling pathway and TG via SERCA inhibition), but not with depolarizing stimulus with high KCl. These data suggest that agonist-induced Ca^{2+} influx is likely due to a functional interaction/communication between TRPC1- and Orai1-dependent SOCC and $Ca_V1.2$ channels in VSMC. Recently, independent studies showed that Orai1 associates with other channels to form the arachidonate-regulated Ca^{2+} (ARC) channels (36), associates with TRPC1 to form non-selective SOCC (8, 37), or even associates with small conductance Ca^{2+}-activated potassium channel 3 (SK3) (11). Therefore, we provided several lines of evidence demonstrating that the SOCC components, Orai1 and TRPC1, form a macromolecular complex with $Ca_V1.2$ LTCC to regulate $[Ca^{2+}]_i$ signaling and vascular tone.

Experimental Procedures

Ethical Approval—All experiments were conducted in accordance with the Spanish legislation on protection of animals (Royal Decree 53/2013), conformed to the Directive 2010/63/EU of the European Parliament, and were approved by the local Ethics Committee of Animal Care of the University Hospital Virgen del Rocío (HUVR) of Seville. Mice (strain C57BL/6) were sacrificed by intraperitoneal administration of a lethal dose of sodium thiopental (200 mg/kg).

$Ca_V1.2^{KO}$ Mouse Model—We used WT and $Ca_V1.2^{KO}$ mice generated at the Institut für Pharmakologie und Toxikologie, München, Germany (17, 23). $Ca_V1.2^{KO}$ mice express a tamoxifen-inducible Cre recombinase under control of the SM22 promoter (SM-Cre ERT2(ki)). To induce smooth muscle-specific Cre recombination, adult mice were treated with freshly prepared tamoxifen solution dissolved in corn oil at 10 mg/ml (Sigma) by intraperitoneal injection once a day for 5 days at a dosage of 1 mg/day. $Ca_V1.2^{KO}$ mice were analyzed between 16 and 18 days after the first injection of tamoxifen, as these animals die between 18 and 21 days (23). The background mouse strain was C57BL/6.

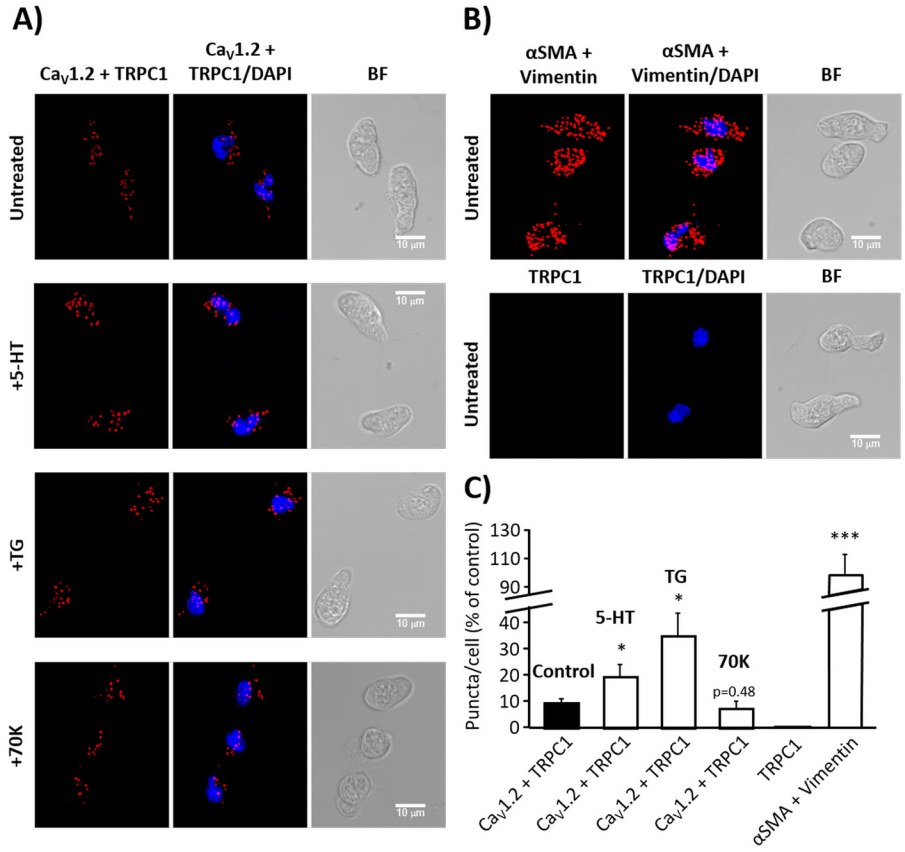

FIGURE 9. **TRPC1 and $Ca_V1.2$ co-localization in aortic myocytes.** *A*, representative images of aortic VSMC using primary antibodies against $Ca_V1.2$ and TRPC1 conjugated with the appropriate PLA probes, from untreated control cells or from cells stimulated with 5-HT (10 μM), TG (2 μM), or high KCl (*70K*, 70 mM). *Red puncta* indicate that proteins are in close proximity (<40 nm). The *left panels* show VSMC images when antibodies were conjugated with PLA probes, the *middle panels* show merge images from cells also stained with DAPI (*blue*), and the *right panels* show bright field (*BF*) pictures. *B*, images from VSMC using primary antibodies against α-SMA and vimentin used as positive control (*upper panel*) and from VSMC conjugated with only anti-TRPC1 primary antibody as negative control (*lower panel*). *C*, the bar graph summarizes the mean number of PLA signals in control VSMC (9.85% ± 1.53; $n = 9$), and in 5-HT- (19.98% ± 4.72; $n = 8$), TG- (35.53% ± 8.78; $n = 9$), or 70K- (7.72% ± 2.76; $n = 4$) treated VSMC. No detectable PLA puncta were observed in control experiments using cells conjugated only with anti-TRPC1 antibody (*TRPC1*, $n = 10$). The interaction between anti-α-SMA and anti-vimentin antibodies was used as positive control (100% ± 14.63; $n = 7$). Similar experiments were repeated 3 times. Values are the percentage of mean ± S.E., normalized to positive control. Significance values indicate difference as compared with control, *, $p < 0.05$, ***, $p < 0.001$.

Measurement of Contractility in Arterial Rings—Thoracic aorta was quickly removed and placed in ice-cold Krebs solution (in mM: 118.5 NaCl, 4.7 KCl, 2.5 $CaCl_2$, 24.8 $NaHCO_3$, 1.2 $MgSO_4$, 1.2 KH_2PO_4, 10 glucose). Then, aorta was cleaned from connective tissue, cut in rings (~2 mm), and mounted on a small-vessel myograph (J.P. Trading, Aarhus, Denmark) to measure isometric tension connected to a digital recorder (Myodataq-2.01, Myodata-2.02 Multi-Myograph System) as described previously (5). Aorta rings were placed on a chamber filled with Krebs solution at 37 °C bubbled with 95% O_2 and 5% CO_2. Before the experiments, segments were subjected to a basal tension of 2.5 micronewtons and stabilized for at least 1 h. The endothelium was mechanically removed by rubbing the luminal surface of the ring with a small plastic tube, and the integrity of the endothelium was tested at the beginning of each experiment by the addition of acetylcholine (up to 10 μM) as described previously (38). The data summary presented in bar graphs shows normalized responses of the increment and the difference between the maximum contraction and resting tone of the vasoconstriction.

Preparation of Aortic Smooth Muscle Cells—The segment of thoracic aorta was quickly removed and placed in cold physiological solution (PS) (in mM: 137 NaCl, 5.4 KCl, 0.2 $CaCl_2$, 4.17 $NaHCO_3$, 2 $MgCl_2$, 0.44 KH_2PO_4, 0.42 NaH_2PO_4, 10 HEPES, 11.11 glucose, 0.05 EGTA). Aorta was dissected, cleaned, cut into pieces, and incubated with 1–2 mg/ml elastase (4 units/mg) and 4 mg/ml collagenase type I (125 units/mg) (Sigma) in PS for 1 h at 4 °C and then for 10–15 min at 37 °C. Cells were mechanically dispersed using fire-polished glass pipettes and plated on coverslips. VSMC were easily distinguished by their size and typical elongated shape, and samples from dispersed cells were stained with mouse anti-α-SMA antibody (Sigma) or phalloidin (Sigma), a marker for F-actin, to verify preparation of VSMC and to rule out any major presence of fibroblasts or endothelial cells.

Cytosolic Ca^{2+} Measurement—VSMC plated on coverslips were incubated in PS with 2–5 μM Fura-2AM for 30 min at room temperature, and then cells were washed. For the experiments, a coverslip was placed on the stage of Nikon Eclipse TS-100 inverted microscope equipped with a 20× Fluor objective (0.75 NA), as described previously (5). Fluorescence images from a large number of loaded single cells were recorded and analyzed with a digital fluorescence imaging system (InCyt Basic Im2, Image Solutions (UK) Ltd., Preston, UK) equipped

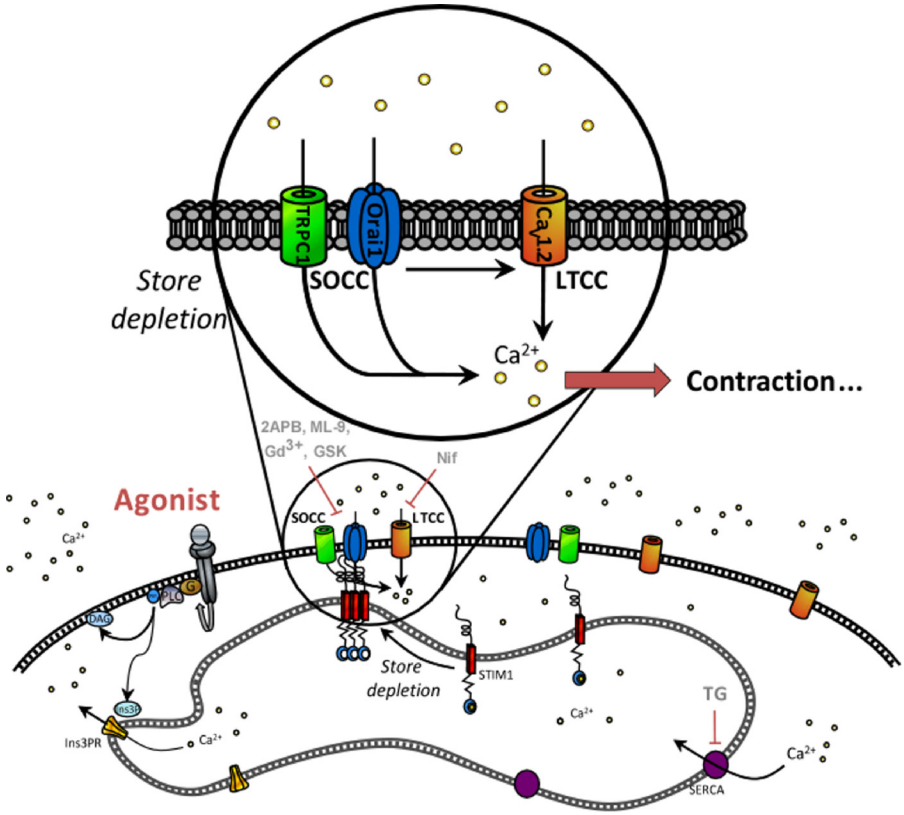

FIGURE 10. **Schematic model summarizing Orai1, TRPC1, and $Ca_V1.2$ co-activation upon 5-HT stimulation.** We propose that 5-HT binding to its receptors promotes $InsP_3$-induced Ca^{2+} release, depletion of Ca^{2+} stores, activation of Ca^{2+} entry through Orai1, and TRPC1-dependent SOCC. The consequent SOCE will trigger secondary activation of LTCC, allowing a significant increase in intracellular free Ca^{2+} concentration and further aorta contraction.

with a light-sensitive CCD camera (Cooke PixelFly, Applied Scientific Instrumentation, Eugene, OR). Changes in $[Ca^{2+}]_i$ are represented as the ratio of Fura-2 fluorescence induced at an emission wavelength of 510 nm due to excitation at 340 and 380 nm (ratio = F_{340}/F_{380}). Ca^{2+} influx was calculated as the difference between the peak ratio before and after the addition of different drugs (Δratio). Data summaries are normalized to control values obtained in each cell preparation as indicated in the figure legends. Auto-fluorescence was determined at the end of each experiment by the addition of ionomycin and $MnCl_2$. Experiments were performed using a continuous perfusion system in physiological salt solution (in mM, pH = 7.4: 140 NaCl, 2.5 $CaCl_2$, 2.7 KCl, 1 $MgCl_2$, 10 HEPES, 10 Glucose). High KCl solution was also used (in mM, pH = 7.4: 70 NaCl, 2.5 $CaCl_2$, 70 KCl, 1 $MgCl_2$, 10 HEPES, 10 glucose).

Protein Extraction and Western Blotting—Dissected arteries from mice were flash-frozen in an ice-cold mixture of 10% TCA and 10 mM DTT in acetone. Arteries were later washed in ice-cold acetone containing 10 mM DTT and lyophilized overnight. Prior to protein extraction, the lyophilized vessels were weighted in an ultra-precision scale to normalize the Western blotting load. 1 μl of sample buffer (60 mM Tris HCl, pH 6.8, 10% glycerol, 2% SDS, 0.01% bromphenol blue, 100 mM DTT) was added for each 2 μg of artery for protein extraction. Samples were heated at 95 °C for 10 min and rotated overnight at 4 °C prior to electrophoresis. Similar amounts of protein samples extracted from WT and $Ca_V1.2^{KO}$ mice were subjected to SDS-PAGE (10%) and electro-transferred onto nitrocellulose membranes. After blocking with 5% nonfat dry milk dissolved in Tris-buffered saline containing 0.1% Tween 20 (TTBS) for 2 h at room temperature, Western blots were probed overnight at 4 °C or for 1.5 h at room temperature with specific primary antibodies in blocking solution. After washing, membranes were incubated for 1 h at room temperature with a horseradish peroxidase-conjugated anti-rabbit or anti-mouse IgG (Jackson ImmunoResearch Laboratories) in TTBS. Detection was performed with the enhanced chemiluminescence reagent ECL Plus (Amersham Biosciences) and the ImageQuant LAS 4000 Mini Gold system. Primary antibodies used were: rabbit anti-$Ca_V1.2$ (1:200, Alomone Labs) and mouse anti-α-tubulin (1:5000, Sigma) as housekeeping loading control. For quantification, tiff images were analyzed with ImageJ software.

In Situ Proximity Ligation Assay—Spatial co-localization of $Ca_V1.2$ and Orai1 were analyzed with PLA technology in freshly isolated aortic myocytes using the Duolink *in situ* PLA detection kit Red (Sigma), following the manufacturer's instructions. VSMC were seeded in a six-channel μ-Slide from IBIDI and fixed with 100% cold methanol for 5 min. VSMC were blocked for 30 min with 3% heat-inactivated goat serum and 1% BSA in PBS and incubated with primary antibodies (rabbit anti-$Ca_V1.2$, 1:50 (Alomone Labs); mouse anti-Orai1, 1:100 (Novus Biologicals); or mouse anti-TRPC1 1:50 in blocking solution (Santa Cruz Biotechnology)) for 2 h at room temperature. Cells were labeled with Duolink PLA anti-rabbit PLUS and anti-mouse MINUS probes for 1 h at 37 °C. The secondary antibod-

ies of PLA PLUS and MINUS probes were attached to synthetic oligonucleotides that hybridize when they are in close proximity (*i.e.* <40 nm separation). The hybridized oligonucleotides were then ligated for 30 min at 37 °C prior to rolling circle amplification for 100 min at 37 °C. Fluorescently labeled oligonucleotides hybridized to the rolling circle amplification product. The red fluorescent fluorophore-tagged oligonucleotides were visualized using a confocal microscope (Leica TCS SP2). Maximum intensity projections of all z-sections (0.5 μm) were obtained by ImageJ software, and puncta of maximum intensity projections were analyzed by Duolink ImageTool software (Sigma). The interaction between anti-α-SMA and anti-vimentin antibodies was used as positive control (Fig. 8*B*). As a negative control, we conducted experiments using only one primary antibody (mouse anti-Orai1 or anti-TRPC1 antibodies), which did not show any detectable PLA signal (Fig. 8*C*).

Confocal Acquisition—Direct confocal acquisition of fluorescence was performed using a Leica TCS SP2 microscope (Leica) equipped with a blue diode at 405 nm, argon-krypton at 458–514 nm, helium-neon at 543 nm, and helium-neon at 633 nm. Images were acquired using a HCX Pl Apo CS 63×/1.3 immersion objective in z-stack intervals of 0.5 μm. Confocal acquisition of fluorescence labels was performed as follows: DAPI (excited at 405 nm and recorded on 400–450 nm) and Alexa Fluor 594 (excited at 594 nm and recorded at 593–667 nm). All figures were processed and mounted by ImageJ software (ConfocalUniovi 1.5 ImageJ), and image deconvolution was conducted using an ImageJ plugin for spectral image deblurring (Parallel Spectral Deconvolution) based on a generalized Tikhonov regularization method (39).

Drugs—Drugs were purchased from Sigma, Invitrogen, and Aobious. The concentration of some inhibitors tested in this study varied when they were used in vessels or cells, but all were within the range of their optimum effects. Higher concentrations were used in rings to ensure inhibitor permeability in thick aorta.

Statistical Analysis—Data analysis was carried out using SigmaPlot software, version 11.0. A sample size calculation was performed prior to the start of this study. We expected a decrease of ~50–100% in vasoreactivity using $Ca_V1.2^{KO}$ mice. We decided to include at least 3–5 subjects for each experiment, taking into consideration an α of 5% and power of 90% or an α of 1% and power of 80% and keeping in mind the failed experiments. Statistical analyses were performed by Student's *t* test for two-group comparison or one-way analysis of variance followed by Tukey multiple comparison post hoc tests comparing different groups. Group data are presented as the percentage of mean ± S.E. and *p* values < 0.05, <0.01, and <0.001 were considered significant as indicated in the figures with *, **, and ***, respectively.

Author Contributions—J. A. M., E. C. S., P. G. R., and T. S. conceived and designed experiments. J. A. M., E. C. S., P. G. R., F. M. Q., J. A. R., A. C., and T. S. collected, analyzed, and interpreted data. F. M. Q., J. A. R., A. C., A. O., and T. S. drafted the article or revised it critically for important intellectual content. All authors approved the final version for publication.

References

1. Catterall, W. A. (2011) Voltage-gated calcium channels. *Cold Spring Harb. Perspect. Biol.* **3,** a003947
2. Bolton, T. B. (1979) Mechanisms of action of transmitters and other substances on smooth muscle. *Physiol. Rev.* **59,** 606–718
3. Parekh, A. B., and Putney, J. W., Jr. (2005) Store-operated calcium channels. *Physiol. Rev.* **85,** 757–810
4. Smani, T., Zakharov, S. I., Csutora, P., Leno, E., Trepakova, E. S., and Bolotina, V. M. (2004) A novel mechanism for the store-operated calcium influx pathway. *Nat. Cell Biol.* **6,** 113–120
5. Smani, T., Domínguez-Rodríguez, A., Hmadcha, A., Calderón-Sánchez, E., Horrillo-Ledesma, A., and Ordóñez, A. (2007) Role of Ca^{2+}-independent phospholipase A_2 and store-operated pathway in urocortin-induced vasodilatation of rat coronary artery. *Circ. Res.* **101,** 1194–1203
6. Smani, T., Patel, T., and Bolotina, V. M. (2008) Complex regulation of store-operated Ca^{2+} entry pathway by PKC-ϵ in vascular SMCs. *Am. J. Physiol. Cell Physiol.* **294,** C1499–C1508
7. Hogan, P. G., and Rao, A. (2015) Store-operated calcium entry: mechanisms and modulation. *Biochem. Biophys. Res. Commun.* **460,** 40–49
8. Rodríguez-Moyano, M., Díaz, I., Dionisio, N., Zhang, X., Avila-Medina, J., Calderón-Sánchez, E., Trebak, M., Rosado, J. A., Ordóñez, A., and Smani, T. (2013) Urotensin-II promotes vascular smooth muscle cell proliferation through store-operated calcium entry and EGFR transactivation. *Cardiovasc. Res.* **100,** 297–306
9. Cheng, K. T., Ong, H. L., Liu, X., and Ambudkar, I. S. (2011) Contribution of TRPC1 and Orai1 to Ca^{2+} entry activated by store depletion. *Adv. Exp. Med. Biol.* **704,** 435–449
10. Kwan, H. Y., Shen, B., Ma, X., Kwok, Y. C., Huang, Y., Man, Y. B., Yu, S., and Yao, X. (2009) TRPC1 associates with BK_{Ca} channel to form a signal complex in vascular smooth muscle cells. *Circ. Res.* **104,** 670–678; Correction (2009) *Circ. Res.* **105**, e6
11. Song, K., Zhong, X. G., Xia, X. M., Huang, J. H., Fan, Y. F., Yuan, R. X., Xue, N. R., Du, J., Han, W. X., Xu, A. M., and Shen, B. (2015) Orai1 forms a signal complex with SK3 channel in gallbladder smooth muscle. *Biochem. Biophys. Res. Commun.* **466,** 456–462
12. Spinelli, A. M., and Trebak, M. (2016) Orai channel-mediated Ca^{2+} signals in vascular and airway smooth muscle. *Am. J. Physiol. Cell Physiol.* **310,** C402–413
13. Beech, D. J. (2012) Orai1 calcium channels in the vasculature. *Pflugers Arch.* **463,** 635–647
14. Smani, T., Hernández, A., Ureña, J., Castellano, A. G., Franco-Obregón, A., Ordoñez, A., and López-Barneo, J. (2002) Reduction of Ca^{2+} channel activity by hypoxia in human and porcine coronary myocytes. *Cardiovasc Res.* **53,** 97–104
15. Derler, I., Schindl, R., Fritsch, R., Heftberger, P., Riedl, M. C., Begg, M., House, D., and Romanin, C. (2013) The action of selective CRAC channel blockers is affected by the Orai pore geometry. *Cell Calcium* **53,** 139–151
16. Bird, G. S., DeHaven, W. I., Smyth, J. T., and Putney, J. W., Jr. (2008) Methods for studying store-operated calcium entry. *Methods* **46,** 204–212
17. Fernández-Tenorio, M., González-Rodríguez, P., Porras, C., Castellano, A., Moosmang, S., Hofmann, F., Ureña, J., and López-Barneo, J. (2010) Short communication: genetic ablation of L-type Ca^{2+} channels abolishes depolarization-induced Ca^{2+} release in arterial smooth muscle. *Circ. Res.* **106,** 1285–1289
18. He, X. D., and Goyal, R. K. (2012) CaMKII inhibition hyperpolarizes membrane and blocks nitrergic IJP by closing a Cl^- conductance in intestinal smooth muscle. *Am. J. Physiol. Gastrointest. Liver Physiol.* **303,** G240–G246
19. Tanner, M. K., and Wellhausen, S. R. (1998) Flow cytometric detection of fluorescent redistributional dyes for measurement of cell transmembrane potential. *Methods Mol. Biol.* **91,** 85–95
20. Rampe, D., and Dage, R. C. (1992) Functional interactions between two Ca^{2+} channel activators, (S)-Bay K 8644 and FPL 64176, in smooth muscle. *Mol. Pharmacol.* **41,** 599–602
21. Domínguez-Rodríguez, A., Díaz, I., Rodríguez-Moyano, M., Calderón-Sánchez, E., Rosado, J. A., Ordóñez, A., and Smani, T. (2012) Urotensin-II

signaling mechanism in rat coronary artery: role of STIM1 and Orai1-dependent store operated calcium influx in vasoconstriction. *Arterioscler. Thromb. Vasc. Biol.* **32,** 1325–1332
22. Park, K. M., Trucillo, M., Serban, N., Cohen, R. A., and Bolotina, V. M. (2008) Role of $iPLA_2$ and store-operated channels in agonist-induced Ca^{2+} influx and constriction in cerebral, mesenteric, and carotid arteries. *Am. J. Physiol. Heart Circ. Physiol.* **294,** H1183–1187
23. Moosmang, S., Schulla, V., Welling, A., Feil, R., Feil, S., Wegener, J. W., Hofmann, F., and Klugbauer, N. (2003) Dominant role of smooth muscle L-type calcium channel $Ca_V1.2$ for blood pressure regulation. *EMBO J.* **22,** 6027–6034
24. Bolotina, V. M. (2012) Orai1, STIM1, and $iPLA_2\beta$ determine arterial vasoconstriction. *Arterioscler. Thromb. Vasc. Biol.* **32,** 1066–1067
25. Nelson, M. T., and Quayle, J. M. (1995) Physiological roles and properties of potassium channels in arterial smooth muscle. *Am. J. Physiol.* **268,** C799–C822
26. Funabashi, K., Ohya, S., Yamamura, H., Hatano, N., Muraki, K., Giles, W., and Imaizumi, Y. (2010) Accelerated Ca^{2+} entry by membrane hyperpolarization due to Ca^{2+}-activated K+ channel activation in response to histamine in chondrocytes. *Am. J. Physiol. Cell Physiol.* **298,** C786–797
27. Noble, D., Borysova, L., Wray, S., and Burdyga, T. (2014) Store-operated Ca^{2+} entry and depolarization explain the anomalous behaviour of myometrial SR: effects of SERCA inhibition on electrical activity, Ca^{2+} and force. *Cell Calcium* **56,** 188–194
28. Dionisio, N., Smani, T., Woodard, G. E., Castellano, A., Salido, G. M., and Rosado, J. A. (2015) Homer proteins mediate the interaction between STIM1 and $Ca_V1.2$ channels. *Biochim. Biophys. Acta* **1853,** 1145–1153
29. Wang, Y., Deng, X., Mancarella, S., Hendron, E., Eguchi, S., Soboloff, J., Tang, X. D., and Gill, D. L. (2010) The calcium store sensor, STIM1, reciprocally controls Orai and $Ca_V1.2$ channels. *Science* **330,** 105–109
30. Hofmann, F., Flockerzi, V., Kahl, S., and Wegener, J. W. (2014) L-type $Ca_V1.2$ calcium channels: from *in vitro* findings to *in vivo* function. *Physiol. Rev.* **94,** 303–326
31. Barrett, C. F., and Tsien, R. W. (2008) The Timothy syndrome mutation differentially affects voltage- and calcium-dependent inactivation of $Ca_V1.2$ L-type calcium channels. *Proc. Natl. Acad. Sci. U.S.A.* **105,** 2157–2162
32. Saponara, S., Sgaragli, G., and Fusi, F. (2008) Quercetin antagonism of Bay K 8644 effects on rat tail artery L-type Ca^{2+} channels. *Eur. J. Pharmacol.* **598,** 75–80
33. Vaca, L. (2010) SOCIC: the store-operated calcium influx complex. *Cell Calcium* **47,** 199–209
34. Berna-Erro, A., Redondo, P. C., and Rosado, J. A. (2012) Store-operated Ca^{2+} entry. *Adv. Exp. Med. Biol.* **740,** 349–382
35. Söderberg, O., Leuchowius, K. J., Gullberg, M., Jarvius, M., Weibrecht, I., Larsson, L. G., and Landegren, U. (2008) Characterizing proteins and their interactions in cells and tissues using the *in situ* proximity ligation assay. *Methods* **45,** 227–232
36. Mignen, O., Thompson, J. L., and Shuttleworth, T. J. (2009) The molecular architecture of the arachidonate-regulated Ca^{2+}-selective ARC channel is a pentameric assembly of Orai1 and Orai3 subunits. *J. Physiol.* **587,** 4181–4197
37. Desai, P. N., Zhang, X., Wu, S., Janoshazi, A., Bolimuntha, S., Putney, J. W., and Trebak, M. (2015) Multiple types of calcium channels arising from alternative translation initiation of the Orai1 message. *Science signaling* **8,** ra74
38. Smani, T., Calderon, E., Rodriguez-Moyano, M., Dominguez-Rodriguez, A., Diaz, I., and Ordóñez, A. (2011) Urocortin-2 induces vasorelaxation of coronary arteries isolated from patients with heart failure. *Clin. Exp. Pharmacol. Physiol.* **38,** 71–76
39. Hansen, P. C., Nagy, J. G., and O'Leary, D. P. (2006) *Deblurring Images: Matrices, Spectra, and Filtering*, Society for Industrial and Applied Mathematics (SIAM), Philadelphia, PA